MicroRNA-223 is a crucial mediator of PPARγ-regulated alternative macrophage activation

Wei Ying,[1] Alexander Tseng,[2] Richard Cheng-An Chang,[3] Andrew Morin,[3] Tyler Brehm,[4] Karen Triff,[5] Vijayalekshmi Nair,[3] Guoqing Zhuang,[3] Hui Song,[6] Srikanth Kanameni,[3] Haiqing Wang,[3] Michael C. Golding,[3] Fuller W. Bazer,[1] Robert S. Chapkin,[7] Stephen Safe,[3] and Beiyan Zhou[3]

[1]Department of Animal Science, Texas A&M University, College Station, Texas, USA. [2]College of Medicine, Texas A&M Health Science Center, College Station, Texas, USA. [3]Department of Veterinary Physiology and Pharmacology, College of Veterinary Medicine and Biomedical Sciences, [4]Department of Chemistry, and [5]Department of Biochemistry, Texas A&M University, College Station, Texas, USA. [6]Department of Physiology, School of Basic Medical Sciences, Wuhan University, Wuhan, Hubei, China. [7]Department of Nutrition and Food Science, Texas A&M University, College Station, Texas, USA.

Polarized activation of adipose tissue macrophages (ATMs) is crucial for maintaining adipose tissue function and mediating obesity-associated cardiovascular risk and metabolic abnormalities; however, the regulatory network of this key process is not well defined. Here, we identified a PPARγ/microRNA-223 (miR-223) regulatory axis that controls macrophage polarization by targeting distinct downstream genes to shift the cellular response to various stimuli. In BM-derived macrophages, PPARγ directly enhanced miR-223 expression upon exposure to Th2 stimuli. ChIP analysis, followed by enhancer reporter assays, revealed that this effect was mediated by PPARγ binding 3 PPARγ regulatory elements (PPREs) upstream of the pre–miR-223 coding region. Moreover, deletion of miR-223 impaired PPARγ-dependent macrophage alternative activation in cells cultured ex vivo and in mice fed a high-fat diet. We identified *Rasa1* and *Nfat5* as genuine miR-223 targets that are critical for PPARγ-dependent macrophage alternative activation, whereas the proinflammatory regulator *Pknox1*, which we reported previously, mediated miR-223–regulated macrophage classical activation. In summary, this study provides evidence to support the crucial role of a PPARγ/miR-223 regulatory axis in controlling macrophage polarization via distinct downstream target genes.

Introduction

Macrophages display heterogeneous phenotypes in response to various microenvironmental signals, ranging from proinflammatory M1 activation to antiinflammatory M2 macrophage responses (1, 2). Upon stimulation with Th1 cytokines, LPS, or free fatty acids, macrophages exhibit proinflammatory M1 responses (3, 4), whereas Th2 cytokines, including IL-4 and IL-13, induce antiinflammatory alternative activation of macrophages (M2) (5, 6). In adipose tissue, the composition of adipose tissue macrophages (ATMs) with polarized activation status is critical for maintaining adipose tissues homeostasis. ATMs in lean tissue primarily display M2 activation status; however, under the stress of obesity, ATMs preferentially undergo proinflammatory M1 activation, which propagates a chronic inflammatory status and insulin resistance (7–9). Although considerable effort has been invested in studying the molecular regulatory network governing macrophage-polarized activation, the full picture has not been fully elucidated.

PPARγ, a nuclear transcription factor, is a key regulator in controlling macrophage polarization in both directions, suppressing classic M1 activation and promoting alternative M2 macrophage responses (10–12). Activation of PPARγ in macrophages is essential for the expression of genes controlling the M2 macrophage responses and subsequently acting on the microenvironment, such as the adipose tissue niche (6, 13–16). In addition, PPARγ can act on both adipocytes and macrophages for insulin-sensitizing and inflammation-suppressive effects, including inflammatory cytokine production, fatty acid metabolism, and mitochondrial activities (13–17). Deletion of *Pparg* in ATMs results in increased M1 activation and blunted M2 macrophage responses, which in turn exacerbate adipose tissue inflammation and insulin sensitivity (6).

We recently identified microRNA-223 (miR-223) as an important regulator of macrophage polarization and ATM-mediated obesity-associated tissue inflammation and insulin resistance (18). miR-223–null mice display significantly enhanced inflammation and insulin resistance after high-fat diet (HFD) feeding, effects that are accompanied by elevated macrophage M1 activation and blunted M2 macrophage responses (18). In addition, transplantation analysis further confirms the contribution of miR-223–deficient myeloid cells to obesity-induced phenotypes (18). We further identify *Pknox1* as a bona fide target gene of miR-223, which favors M1 proinflammatory activation in macrophages (18). Given the importance of miR-223 in controlling macrophage polarization, however, it is unclear how its expression is regulated and which genes can mediate miR-223 action in controlling M2 activation in macrophages.

In this study, we demonstrate that miR-223 is required for PPARγ-dependent macrophage alternative activation using both in vivo and ex vivo models. PPARγ can control miR-223 expression by directly binding to the PPARγ regulatory elements (PPREs) located in the *Mir223* promoter. In addition, we demonstrate that *Rasa1* and *Nfat5* are genuine targets of miR-223 and are important for the PPARγ/miR-223 regulatory axis in controlling macrophage alternative activation.

Authorship note: Wei Ying and Alexander Tseng contributed equally to this work.
Conflict of interest: The authors have declared that no conflict of interest exists.
Submitted: February 24, 2015; **Accepted:** August 27, 2015.
Reference information: *J Clin Invest*. 2015;125(11):4149–4159. doi:10.1172/JCI81656.

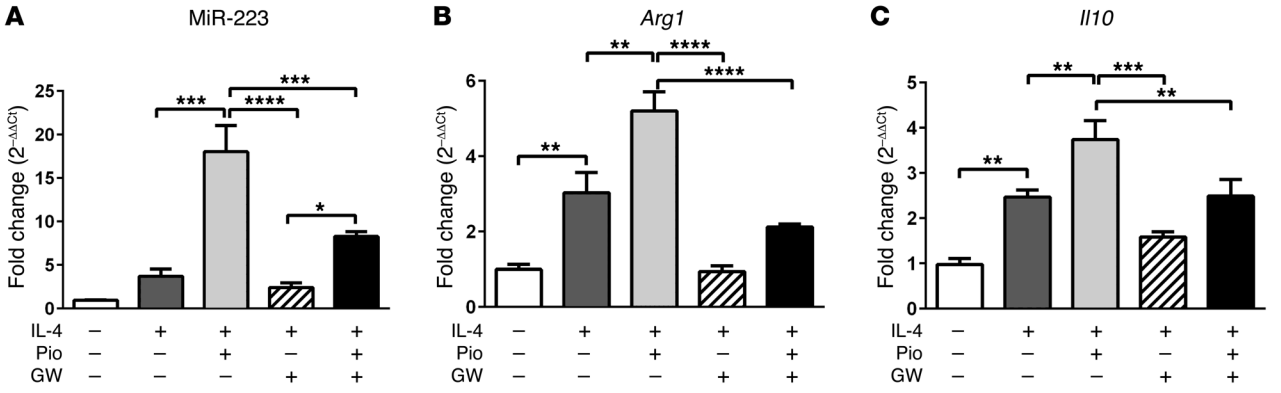

Figure 1. miR-223 expression is induced in PPARγ-dependent M2 macrophage activation. Expression of miR-223 (**A**), arginase 1 (*Arg1*) (**B**), and IL-10 (*Il10*) (**C**) in WT BMDMs in the presence of IL-4 with or without pioglitazone (Pio) or PPARγ antagonist GW9662 (GW) for 48 hours (n = 3). Data are presented as the mean ± SEM. $^{**}P < 0.01$, $^{***}P < 0.001$, and $^{****}P < 0.0001$ by 1-way ANOVA with Bonferroni's post test.

Results

miR-223 deficiency blunts PPARγ-dependent macrophage alternative activation. PPARγ and miR-223 are both potent regulators of macrophage-polarized activation (6, 18). We first examined miR-223 levels during macrophage activation in the presence of the PPARγ agonist pioglitazone. As expected, miR-223 was significantly induced during M2 macrophage activation in BM-derived macrophages (BMDMs) stimulated with IL-4 (Figure 1A and ref. 18). In addition, administration of pioglitazone, an agonist of PPARγ, further enhanced miR-223 expression in M2 macrophages (Figure 1A), which was accompanied by elevated expression of the key M2 activation–related genes arginase 1 (*Arg1*) and *Il10* (Figure 1, B and C). On the other hand, BMDMs stimulated with IL-4 in the presence of GW9662, a PPARγ antagonist, displayed blunted M2 macrophage activation with respect to *Arg1* and *Il10* expression (Figure 1, B and C). More important, induction of miR-223 expression by pioglitazone was diminished in the presence of GW9662 (Figure 1A).

Next, to further confirm that induced miR-223 expression is crucial in mediating PPARγ-dependent macrophage alternative activation, we used both gain and loss of miR-223 strategies in combination with PPARγ agonist administration. BMDMs derived from *Mir223*-KO mice (BMDM-miR223KO) or WT BMDMs transfected with a miR-223 overexpression construct (BMDM-miR223oe) were activated by IL-4 with or without the administration of pioglitazone, and the activation-related features were examined after 48 hours of stimulation. Indeed, loss of miR-223 displayed blunted M2 macrophage activation as demonstrated previously (18), and this defect was not fully rescued by pioglitazone treatment as evidenced by decreased levels of the activation-related surface marker CD69 and other key genes such as peroxisome proliferator–activated receptor γ, coactivator 1 α (*Pgc1a*), *Il10*, and *Arg1* (Figure 2, A and B). Conversely, overexpression of miR-223 in WT BMDMs enhanced M2 macrophage responses (oe–IL-4 vs. ev–IL-4; Figure 2C), which was similar to the improvement observed for expression of the activation-related surface marker CD69 in WT BMDMs induced by pioglitazone treatment (oe–IL-4 vs. ev–IL-4 + pio; Figure 2C). Further, pioglitazone treatment increased the expression of the activation-related cell surface marker CD69 in these BMDMs with ectopic expression of miR-223 (oe–IL-4 + pio vs. ev–IL-4 + pio; Figure 2C). Ectopic expression of miR-223 also led to enhanced M2 activation–related genes such as *Pgc1a* and *Arg1* in the presence of pioglitazone (Figure 2D). In addition, to evaluate whether overexpression of miR-223 in BMDMs could rescue the inhibitory effect of suppressed PPARγ activity, we subjected the BMDMs with overexpressed miR-223 to GW9662, an antagonist of PPARγ activation, followed by IL-4 stimulation. Interestingly, ectopic expression of miR-223 prevented the suppressive effects of GW9662 on M2 macrophage responses as evidenced by the expression of *Arg1* and *Pgc1a* (Figure 2E). In addition, introducing the miR-223 ectopic expression construct into miR-223–null BMDMs recovered the M2 phenotype in response to IL-4 (Supplemental Figure 1; supplemental material available online with this article; doi:10.1172/JCI81656DS1). Taken together, these results demonstrate that miR-223 is required for PPARγ-dependent M2 macrophage activation.

miR-223 is a crucial mediator of PPARγ action in ATMs. PPARγ can ameliorate obesity-induced metabolic defects by both insulin sensitization and inflammation suppression (19–21). We investigated the potential impact of miR-223 deficiency in mediating PPARγ action in the context of obesity using a diet-induced obese mouse model. WT and *Mir223*-KO male mice were fed an HFD from the age of 5 weeks for 16 weeks. During the last 4 weeks of the HFD feeding regimen, mice were also given pioglitazone at a dose of 10 mg/kg/day or saline as a control. At the end of the feeding regimen, all groups were subjected to a glucose tolerance test and insulin tolerance analysis. During the feeding period, there was no significant difference among groups in terms of food intake, BW gain, or adiposity (Supplemental Figure 2). As expected, WT mice that received pioglitazone treatment (HFD-WT-pio; Figure 3, A and B) displayed significantly improved results in both glucose and insulin tolerance tests compared with the HFD-fed WT mice (HFD-WT; Figure 3, A and B). However, such improvement with pioglitazone was significantly compromised in mice with miR-223 deficiency (HFD-miR223KO-pio; Figure 3, A and B). Further analysis also confirmed that pioglitazone exerts less beneficial effects on insulin sensitivity in *Mir223*-KO mice as evidenced by plasma glucose and insulin levels under HFD-fed or fasted conditions and by expression of metabolically related genes (Figure 3, C–E, and Supplemental Figure 3).

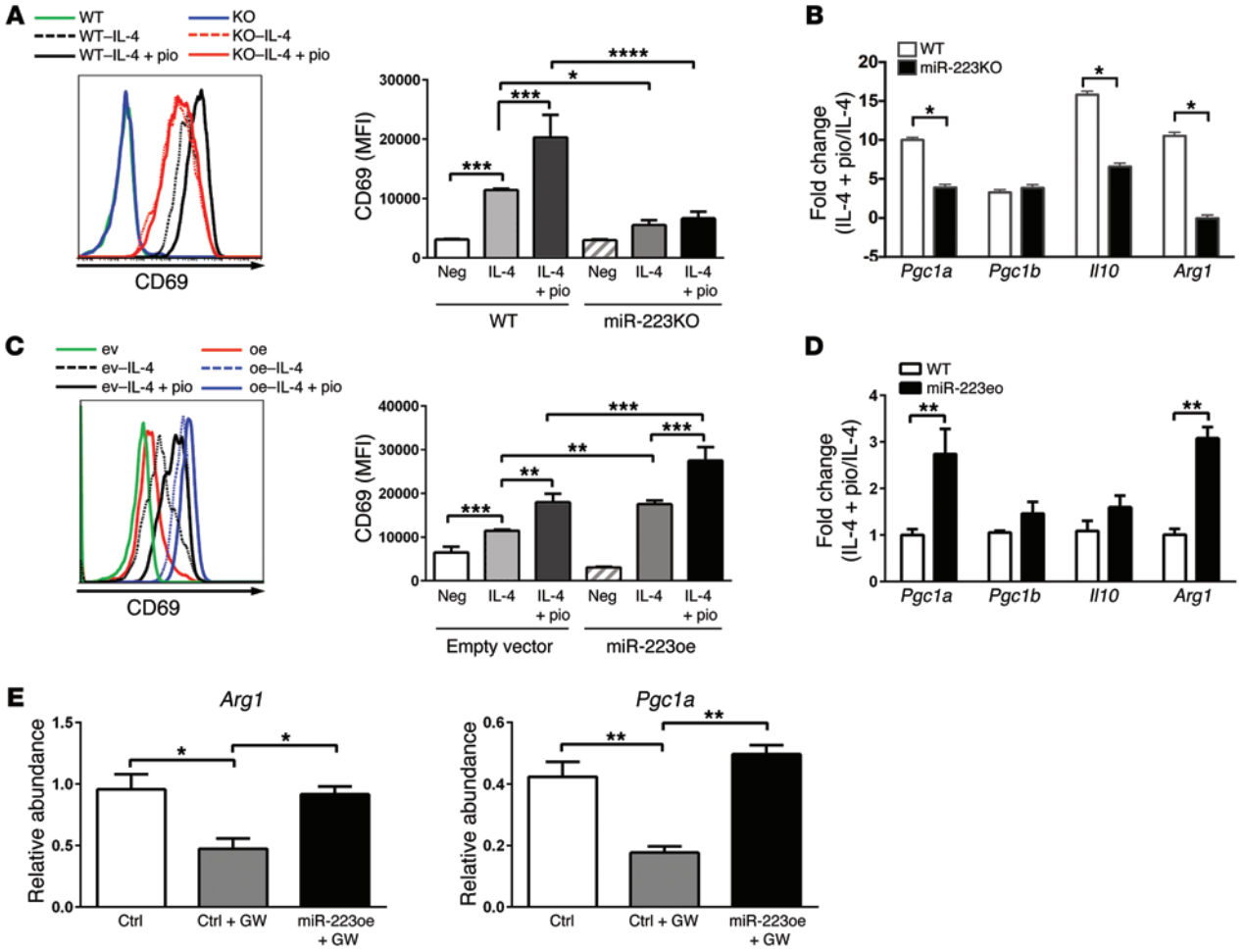

Figure 2. miR-223 is required for PPARγ-dependent M2 macrophage activation. (**A** and **B**) Expression of activation-related surface marker CD69 and M2 response–related genes in WT BMDMs with *Mir223* KO (miR-223KO) upon IL-4 stimulation with or without pioglitazone for 48 hours ($n = 3$). (**C** and **D**) Expression of activation-related surface marker CD69 and M2 response–related genes in WT BMDMs with miR-223 overexpression (miR-223oe) upon IL-4 stimulation with or without pioglitazone for 48 hours. WT BMDMs transfected with empty vector were used as a control ($n = 3$). ev, empty vector; oe, overexpression. (**E**) *Arg1* and *Pgc1a* expression in WT BMDMs with miR-223 overexpression upon IL-4 stimulation with or without the PPARγ antagonist GW9662 for 48 hours ($n = 3$). Ctrl, WT BMDMs transfected with empty vector. Data are presented as the mean ± SEM. $^*P < 0.05$, $^{**}P < 0.01$, $^{***}P < 0.001$, and $^{****}P < 0.0001$ by 1-way ANOVA with Bonferroni's post test (**A**, **C**, and **E**) and Student's *t* test (**B** and **D**). MFI, mean fluorescence intensity; Neg, negative control; pio, pioglitazone.

Consistent with our previous report (18), miR-223 is preferentially expressed in ATMs, but not in adipocytes. Of note, pioglitazone treatment enhanced miR-223 induction in isolated ATMs from HFD-WT mice (Figure 4A), confirming our observation that PPARγ activation induced miR-223 expression in BMDMs (Figure 1A). Given that miR-223 is abundantly expressed in ATMs but at low or nondetectable levels in adipocytes (18), we focused on the phenotypes in ATMs isolated from visceral adipose tissue (VAT) of HFD-fed mice. After 4 weeks of pioglitazone treatment, immunohistochemical analysis of VAT sections showed similar populations of F4/80$^+$ cells located in the VAT of HFD-fed mice with or without pioglitazone treatment (Figure 4B). Flow cytometric analysis also confirmed the comparable proportion of F4/80$^+$CD11b$^+$ ATMs between groups with or without pioglitazone treatment (Figure 4, C and D). As expected, the proportion of M1 (F4/80$^+$CD11b$^+$CD206$^-$CD11c$^+$) cells was significantly lower in mice treated with pioglitazone (HFD-WT-pio) compared with that seen in control (HFD-WT) mice (Figure 4, E and F). We also observed a dramatically increased proportion of M2 (F4/80$^+$CD11b$^+$CD206$^+$CD11c$^-$) cells in HFD-WT-pio mice (Figure 4, E and F). Intriguingly, the inflammation-suppressive and insulin-sensitizing effects of pioglitazone were abolished in *Mir223*-KO mice in terms of ATM M1 cell proportions (Figure 4, E and F, and Supplemental Figure 4), inflammatory cytokine production (Figure 5, A and B), insulin sensitization (Figure 5C and Supplemental Figure 5), and PPARγ-dependent inhibition of NF-κB or JNK activation (Figure 5, D and E). Taken together, our results further demonstrate that miR-223 is a crucial mediator of PPARγ action in controlling ATM function and macrophage alternative activation.

PPARγ regulates miR-223 expression by binding to 3 PPREs in its promoter. Given the inducible expression of miR-223 triggered by PPARγ activation, we surveyed the *Mir223* upstream region for potential PPREs. Using the JASPAR database algorithms (http://jaspar.binf.ku.dk/) (22), we predicted 8 potential classical PPREs (AGG(A/T)CA) (23–25) within 4 kb upstream of the pre–miR-223 coding region. To identify the genuine binding sites, we used ChIP

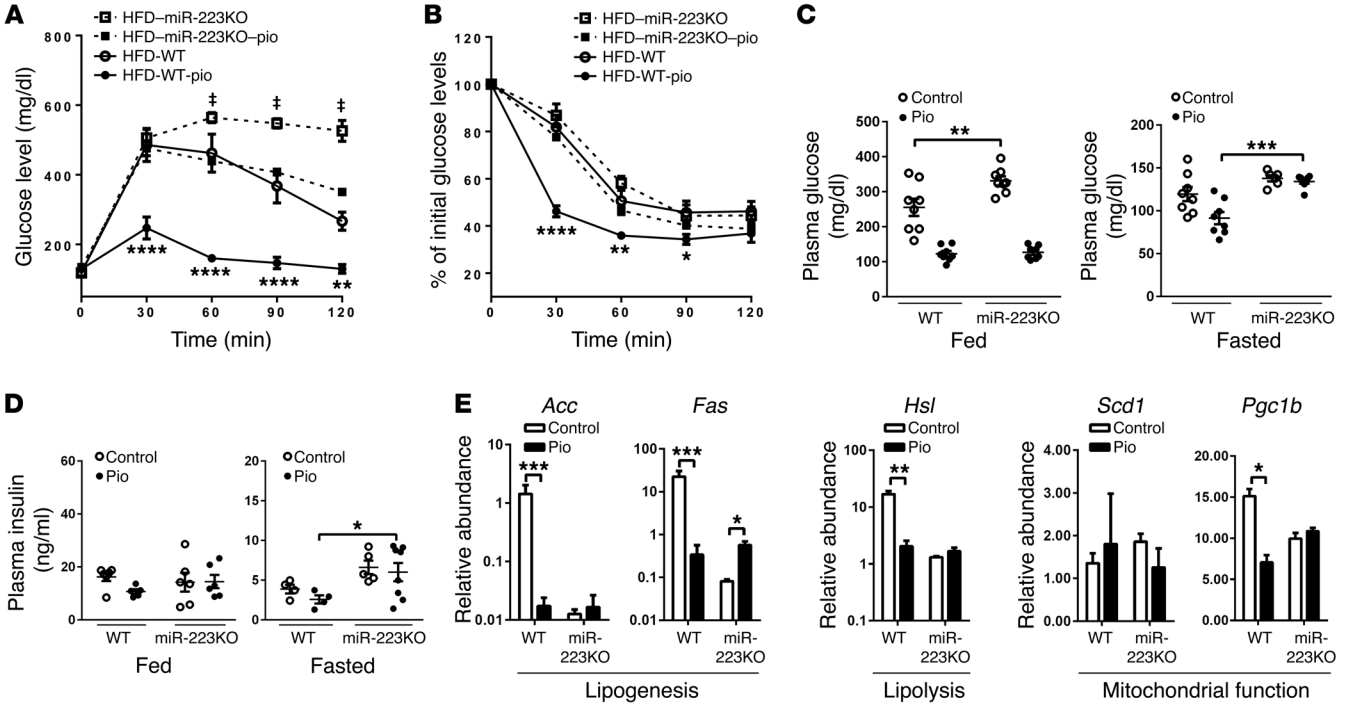

Figure 3. miR-223 deficiency impairs PPARγ-mediated improvement of adipose tissue function under the stress of obesity. (**A** and **B**) Glucose tolerance test and insulin tolerance test (n = 9–10). (**C** and **D**) Glucose and insulin plasma concentrations for WT and *Mir223*-KO mice fed an HFD without (Control) or with pioglitazone (Pio) supplementation or fasted for 16 hours (n = 6–10). (**E**) Expression of key regulators of lipogenesis, lipolysis, and mitochondrial function in VAT of HFD-fed mice with pioglitazone treatment (Pio) or without (Control) (n = 3). *Acc*, acetyl-CoA carboxylase; *Fas*, fatty acid synthetase; *Hsl*, hormone-sensitive lipase; *Scd1*, stearoyl-CoA desaturase-1. Data are presented as the mean ± SEM. $^{‡}P < 0.05$, HFD–miR-223KO versus HFD–miR-223KO–pio; $^{*}P < 0.05$, $^{**}P < 0.01$, $^{***}P < 0.001$, and $^{****}P < 0.0001$, HFD-WT versus HFD-WT-pio by 2-way ANOVA (**A** and **B**), 1-way ANOVA with Bonferroni's post test (**C** and **D**), and Student's t test (**E**).

methodology with Abs against PPARγ in nuclei isolated from naive BMDMs (M0), alternatively activated BMDMs (M2), or M2 cells treated with pioglitazone. The enrichment of PPREs was examined by quantitative PCR (qPCR) with primer pairs flanking each predicted PPRE (Figure 6A). Interestingly, 3 PPREs (–3619 to –3624, –1305 to –1310, and –1011 to –1016, relative to the 5′ end of the pre–miR-223 coding region) displayed enrichment as evidenced by the fold change relative to total DNA input and IgG control (Figure 6A). Enrichment of these 3 PPREs was significantly elevated in M2 cells (Figure 6A). Pioglitazone treatment further enhanced PPARγ recruitment in the pre–miR-223 upstream region compared with that observed in M0 and M2 cells (Figure 6A).

To validate the efficacy of these 3 PPREs in mediating PPARγ-regulated transcription, we inserted the authentic genomic sequences harboring PPREs upstream of the SV40 promoter, followed by a firefly luciferase expression cassette (pGL3 promoter; Figure 6B). Luciferase activity was examined in the murine-derived macrophage cell line RAW264.7 stimulated by IL-4 for M2 macrophage activation. Our results demonstrate that the 3 PPREs with enriched binding efficacy with PPARγ can enhance luciferase activity in alternatively activated macrophages compared with the cells transfected with control vector (Figure 6B). More interestingly, this induced activation could be further enhanced by pioglitazone stimulation (Figure 6B). In contrast, mutation of these PPREs impaired recruitment of PPARγ upstream of pre–miR-223 as evidenced by significantly decreased luciferase activity in response to IL-4 and pioglitazone (Figure 6C). Thus, these results demonstrate that PPARγ can directly regulate miR-223 expression in M2 macrophages through at least 3 PPREs located within 4 kb upstream of the miR-223 precursor sequence.

Rasa1 and Nfat5 are genuine miR-223 target genes and important for M2 macrophage activation. miRs exert their biological functions by either blocking translation and/or inducing degradation of the target mRNAs by base-pairing to the recognition sites (26, 27). We previously identified a prodiabetic gene, *Pknox1*, as a bone fide miR-223 target gene that plays critical roles in modulating the function of miR-223 in macrophages (18). However, both loss and ectopic expression of *Pknox1* primarily altered M1 macrophage activation, with limited impact on M2 macrophages (18). Thus, we screened additional targets and sought genes that are regulated by miR-223 and crucial for M2 macrophage activation. Using prediction algorithms in TargetScan Mouse 6.2 (www.targetscan.org) (28, 29) and luciferase reporter assays, we identified 2 new targets of miR-223, *Rasa1* and *Nfat5,* as evidenced by suppression of their luciferase activity in the presence of miR-223 (Figure 7A). In contrast, mutation of the miR-223–binding site in the 3′-UTR of *Rasa1* and *Nfat5* prevented the inhibition of luciferase activity by miR-223 (Figure 7A). *Nfat5* is a member of the nuclear factors of activated T cells family of transcription factors and plays crucial roles in modulating immune responses (30), and its 3′-UTR harbors 1 conserved 8-mer and 2 nonconserved 7-mer miR-223 sites. *Rasa1* is a member of the GAP1 family of GTPase-activating proteins and

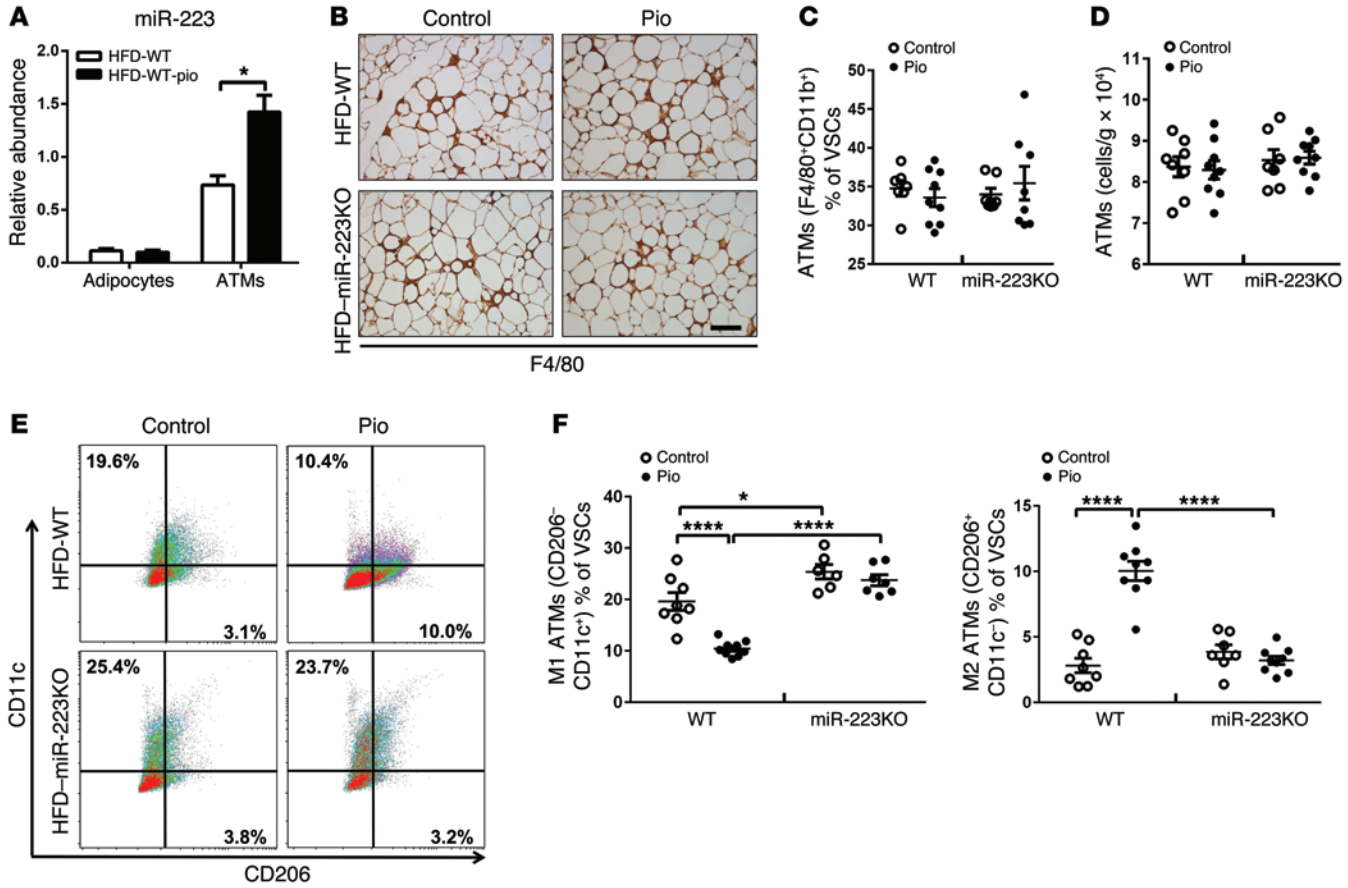

Figure 4. miR-223 deficiency impairs PPARγ-mediated ATM activation. (**A**) Expression pattern of miR-223 in adipocytes and ATMs from HFD-fed WT mice with or without pioglitazone supplementation (n = 3). (**B**–**F**) Population of macrophages (F4/80$^+$CD11b$^+$) and their subtypes in VSCs of VAT from HFD-fed WT or *Mir223*-KO mice (n = 8–9). M1, F4/80$^+$CD11b$^+$CD206$^-$CD11c$^+$; M2, F4/80$^+$CD11b$^+$CD206$^+$CD11c$^-$. Control, mice without pioglitazone treatment; Pio, mice treated with pioglitazone. Scale bar: 100 μm. Data are presented as the mean ± SEM. *P < 0.05 and ****P < 0.0001 by Student's t test (**A**) and 1-way ANOVA with Bonferroni's post test (**C**, **D**, and **F**).

a known component in pathways crucial for immune cell function (31). We evaluated the expression of these genes in activated macrophages. As expected, these 2 genes displayed an inverse correlation with miR-223 in M2 macrophages (Figure 7B), i.e., lower levels in M2 macrophages when miR-223 was induced during alternative activation, and relatively higher levels in *Mir223*-KO macrophages compared with WT cells (Figure 7C). We also observed that mRNA and protein levels of these miR-223 target genes were greater in VAT of HFD-*Mir223*-KO mice compared with those in HFD-WT mice (Figure 7, D and E). Interestingly, the suppression of *Rasa1* and *Nfat5* in M2 cells was enhanced in the presence of pioglitazone (Figure 7B), suggesting the potential roles of these 2 genes in regulating PPARγ/miR-223 alternative macrophage activation.

To understand the function of *Rasa1* and *Nfat5* in mediating PPARγ/miR-223 regulatory axis–controlled macrophage polarization, we performed gain- and loss-of-function analysis. After validating overexpression or knockdown of these genes in *Mir223*-KO BMDMs (Supplemental Figure 6), we subjected the cells to alternative activation by LPS or IL-4 and evaluated the activation features as previously described. *Mir223*-KO BMDMs with decreased levels of *Nfat5* or *Rasa1* exhibited blunted M1 responses upon LPS stimulation (Figure 8, A and B, and Supplemental Figure 7A). In contrast, ectopic expression of *Nfat5* or *Rasa1* enhanced M1 phenotypes (Figure 8, A and B, and Supplemental Figure 7, A and B). Upon IL-4 stimulation, loss of *Nfat5* or *Rasa1* in *Mir223*-KO BMDMs significantly enhanced M2 macrophage activation as evidenced by the dramatically increased expression of activation-related cell-surface marker CD69 (Figure 8, A and B) and *Arg1* (Supplemental Figure 7, C and D). Conversely, *Mir223*-KO BMDMs with ectopic expression of *Nfat5* or *Rasa1* had blunted M2 macrophage responses (Figure 8, A and B, and Supplemental Figure 7, C and D). In addition, knockdown of *Nfat5* or *Rasa1* in *Mir223*-KO BMDMs restored the improvement in M2 macrophage responses induced by pioglitazone (Figure 8, C and D), but had a minor impact on M1 activation in the presence of pioglitazone (Supplemental Figure 8). Taken together, these results demonstrate that *Rasa1* and *Nfat5* are bona fide miR-223 target genes and play critical roles in PPARγ/miR-223 regulatory axis–mediated M2 macrophage activation.

Discussion

Polarization of macrophages is tightly regulated by a well-orchestrated network, and PPARγ plays a central role in controlling macrophage alternative activation (6, 32). In addition, epigenetic regulators, including miRs, exert an additional layer of regulation

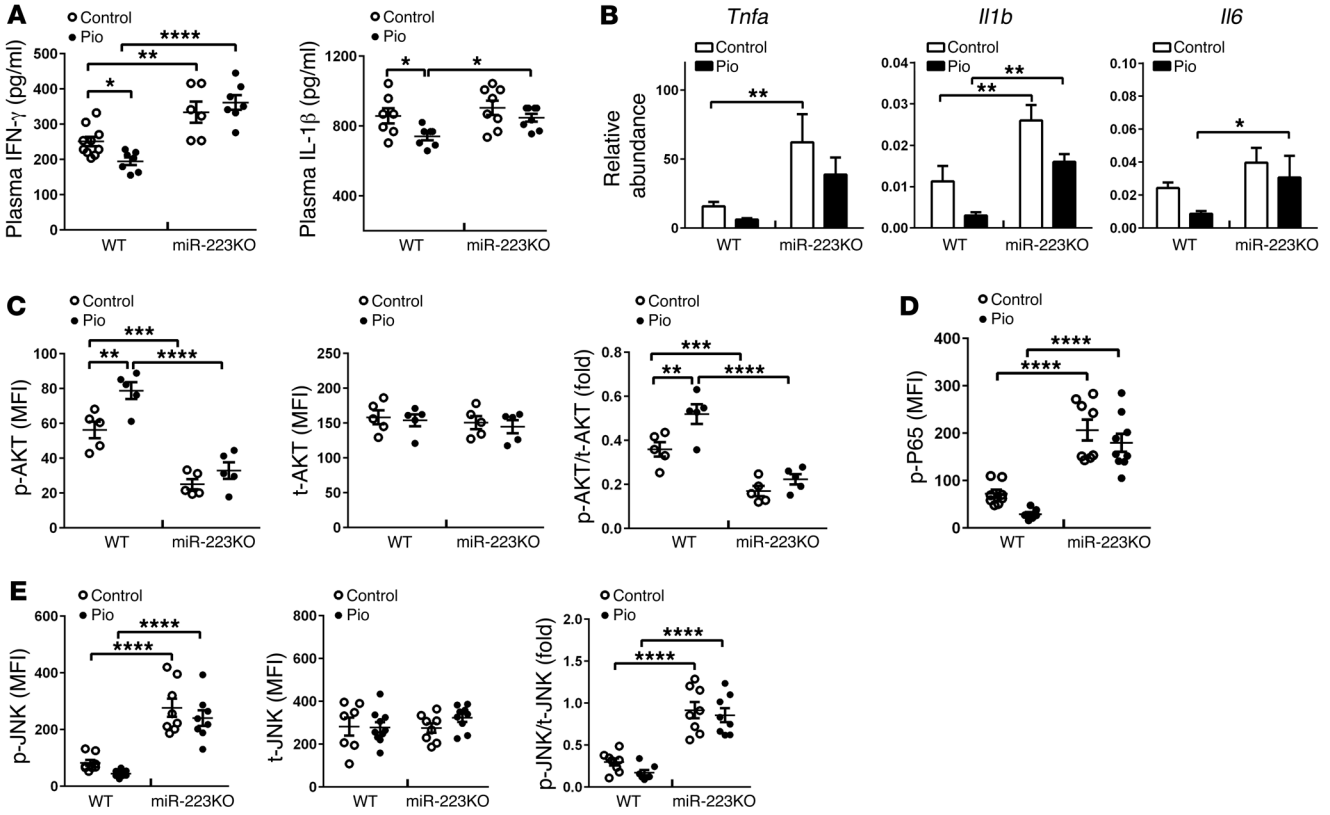

Figure 5. miR-223 deficiency impairs PPARγ functions in modulating adipose tissue functions under obese stress. (**A**) Concentrations of plasma proinflammatory cytokines IFN-γ and IL-1β in HFD-fed mice with pioglitazone (Pio) treatment or without (Control) (n = 6–9). (**B**) Gene expression of inflammatory cytokines TNF-α (*Tnfa*), IL-1β (*Il1b*), and IL-6 (*Il6*) in VAT (n = 3). (**C**) Activation of the AKT-signaling pathway in VAT of HFD mice treated with pioglitazone (HFD-pio) (n = 5). (**D** and **E**) Activation of NF-κB and JNK signaling pathways in VAT of HFD-fed mice (n = 6–9). Control, mice without pioglitazone treatment; Pio, mice treated with pioglitazone; t-, total. Data are presented as the mean ± SEM. $^*P < 0.05$, $^{**}P < 0.01$, $^{***}P < 0.001$, and $^{****}P < 0.0001$ by 1-way ANOVA with Bonferroni's post test.

in the signaling network (33). Our previous study demonstrated that miR-223 is a potent regulator in controlling the polarized activation of macrophage polarization and ATM-mediated tissue inflammation and insulin resistance under the stress of obesity (18). However, the interplay between miRs and PPARγ in controlling macrophage responses is not clear. In this study, we provide evidence to support the crucial roles of the PPARγ/miR-223 axis in modulating macrophage polarization, which is at least partially mediated by *Nfat5* and *Rasa1*. Our findings reveal that PPARγ can promote miR-223 expression in M2 macrophages by directly binding to the PPREs located in the *Mir223* promoter region and that depletion of miR-223 in macrophages greatly impairs PPARγ-dependent alternative M2 macrophage activation.

ATMs exert profound effects on the homeostasis of adipose tissue by responding to the distinct stimuli with heterogeneous activation phenotypes (34–36). M1 ATMs promote chronic inflammation induced by obesity and facilitate the clearance of apoptotic adipocytes (37–39), whereas M2 ATMs are major coordinators of adipose tissue remodeling and repair with antiinflammatory features (40, 41). In the context of obesity, there is a dramatic increase in white adipose tissue infiltration of macrophages, which account for about 40% of the stromal cell population in obese visceral fat depots (3, 9). Moreover, not only do total numbers of ATMs increase, but they also display an increased ratio of M1/M2 status, resulting in overall enhanced inflammation in the VAT, which is a causal factor in the development of systemic insulin resistance (2, 7). Activation of PPARγ can act through inflammation-suppressing and insulin-sensitizing mechanisms to ameliorate the metabolic and immunologic disturbances in obese adipose tissue (19–21). Odegaard et al. reported that KO of macrophage-specific *Pparg* results in impaired M2 responses of ATMs, which subsequently exacerbates obesity-associated insulin resistance (6). In our study, the results demonstrate that enhanced activation of the PPARγ-mediated signaling pathway led to the phenotypical switch from proinflammatory M1 activation to the antiinflammatory M2 response of ATMs. However, we also found that depletion of miR-223 significantly impaired the beneficial effects of PPARγ action in this context, suggesting that miR-223 is a crucial component in the PPARγ regulatory network. Given that the expression of miR-223 is primarily in macrophages but not in adipocytes (Figure 4A) (18), we focused our investigation on macrophages to further interrogate their interplay. A previous study demonstrated decreased ATM populations (42). However, in our study, total ATM numbers were similar in mice with or without pioglitazone supplementation, which may be due to the difference in pioglitazone treatment regimens between the previous study (42) and ours.

Our previous study showed that miR-223 is a potent regulator for macrophage polarization and favors M2 macrophage activation

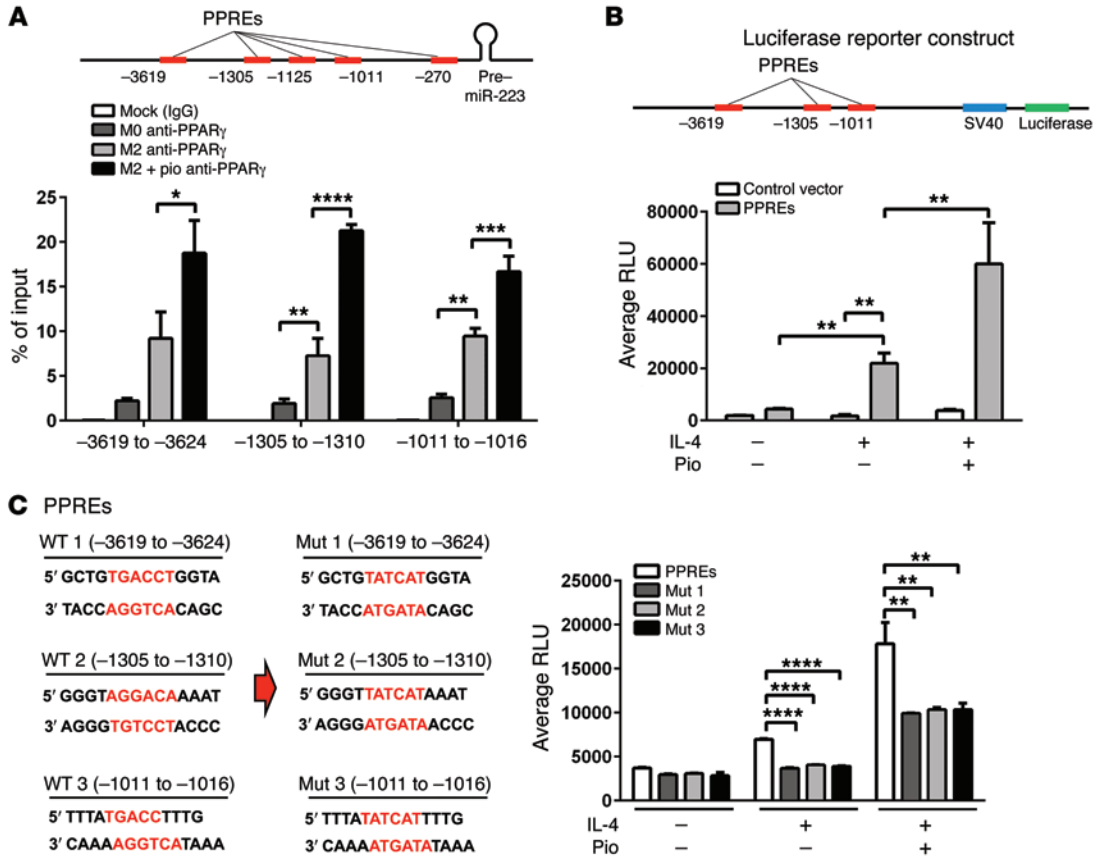

Figure 6. PPARγ regulates miR-223 expression by binding to 3 PPREs in its promoter. (**A**) After ChIP with Abs against PPARγ in naive (M0), IL-4–stimulated (M2), or pioglitazone-treated M2 macrophage cell lysates, the enrichment of potential PPREs upstream of the miR-223 precursor gene (pre–miR-223) were validated by qPCR with tiled primer pairs (n = 4). (**B**) Luciferase activity of the reporter construct harboring the upstream region (–3849 to –978 relative to the 5′ end) of pre–miR-223 or empty vector in the presence of IL-4, with or without pioglitazone for 36 hours (n = 4). (**C**) Site mutation (Mut) of PPREs (n = 4). Data are presented as the mean ± SEM. *P < 0.05, **P < 0.01, ***P < 0.001, and ****P < 0.0001 by 1-way ANOVA with Bonferroni's post test.

(18). To elucidate the role of miR-223 in PPARγ-regulated macrophage alternative activation, we tested the activation profiles of BMDMs with WT, null, or overexpressed miR-223 and the response of these BMDMs to either PPARγ agonist or antagonist. Our results demonstrate that miR-223 is required for PPARγ function and that its deficiency can lead to compromised activation of the BMDM response to IL-4. In addition, in the presence of PPARγ antagonist, overexpression of miR-223 could partially rescue the macrophage alternative activation due to suppression of PPARγ (Figure 2E). Taken together, these results demonstrate the critical role of miR-223 in PPARγ-dependent signaling and its ability to act downstream of PPARγ to modulate M2 macrophage activation. Indeed, we identified 3 PPREs located within 4 kb upstream of the pre–miR-223 coding region and validated their enhancer function using a luciferase reporter assay. We also observed that inhibition of PPARγ action impaired its induction of miR-223 expression in M2 macrophages (Figure 1A), suggesting that *Mir223* is a PPARγ-induced gene.

Our previous study showed that *Pknox1* is a proinflammatory regulator and a genuine miR-223 target gene in macrophages (18). Analysis of both gain and loss of *Pknox1* confirmed the role of miR-223 in modulating classic M1 activation and its limited impact on M2 macrophage responses. Given the crucial role of miR-223 in controlling alternative macrophage activation, we screened an additional pool of genes and identified 2 new target genes, *Nfat5* and *Rasa1*. Both genes were known to be important in regulating immune cell responses (30, 31). NFAT5, a transcription factor and a member of the NFAT family, exhibits important regulatory functions for inflammatory responses by acting on NF-κB signaling pathways (30). The function of RASA1 is tightly regulated to stimulate GTPase activity. In addition, RASA1 plays a critical role in regulating IL-4–induced signaling pathways in T lymphocytes (31). Our luciferase reporter analysis validated that those predicted target elements are responsible for miR-223 action in macrophages, indicating conserved target sites in the 3′-UTRs of *Nfat5* and *Rasa1*. Moreover, miR-223 expression patterns in macrophages were inversely correlated with expression of *Rasa1* and *Nfat5*. Thus, we further examined the function of these genes in controlling macrophage activation and, more importantly, in mediating the PPARγ/miR-223 regulatory axis. Our results demonstrate that *Rasa1* and *Nfat5* are genuine targets of miR-223 and play crucial roles in PPARγ-dependent macrophage alternative activation.

Previous studies reported that long-term (more than 12 weeks) pioglitazone treatment resulted in increased adiposity (43). However, in our study, treatment with pioglitazone for 4 weeks did not affect the BW or adiposity of HFD-fed mice (Supplemental Figure 2), which may be due to the shorter period of pioglitazone treat-

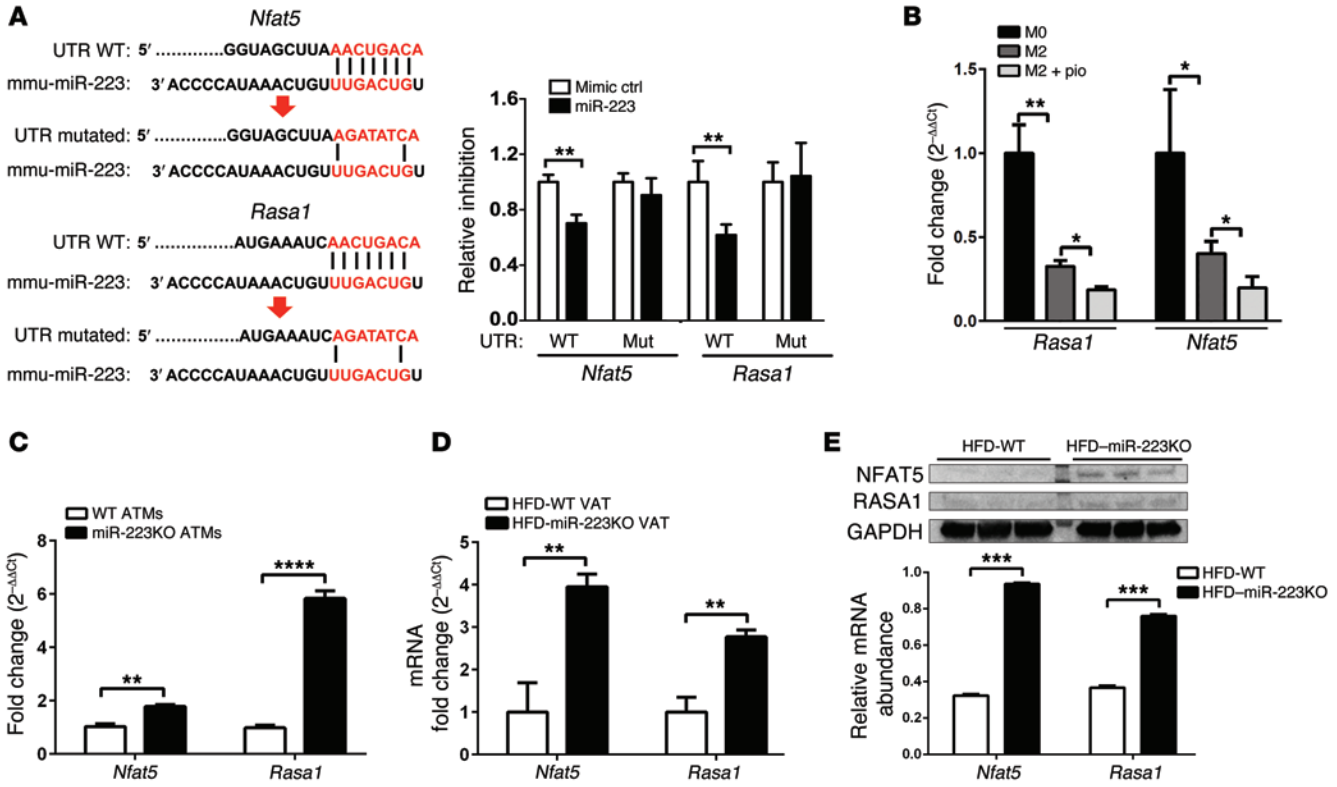

Figure 7. *Rasa1* and *Nfat5* are 2 miR-223 target genes. (**A**) Reporter constructs containing a 3′-UTR with a WT or mutated miR-223–binding site of the target genes (Mut) (n = 3). (**B**) Expression of the miR-223 target genes *Rasa1* and *Nfat5* in M0, M2, or M2 WT BMDMs treated with pioglitazone (n = 3). (**C**) Abundance of *Nfat5* and *Rasa1* in ATMs isolated from WT or miR-223KO lean mice (n = 3). (**D** and **E**) mRNA and protein levels of *Nfat5* and *Rasa1* in VAT of HFD-fed WT and *Mir223*-KO mice, respectively (n = 4). Data are presented as the mean ± SEM. $^*P < 0.05$, $^{**}P < 0.01$, $^{***}P < 0.001$, and $^{****}P < 0.0001$ by Student's t test (**A** and **C**–**E**) and by 1-way ANOVA with Bonferroni's post test (**B**).

ment. Nakamura et al. also reported that there was no change in BW after 4 weeks of pioglitazone treatment (44). Consistent with the previous results (45), we observed improved insulin sensitivity with pioglitazone treatment. Although PPARγ can enhance insulin sensitivity through modulation of macrophage activation, this transcription factor's actions in key metabolic tissues such as adipose tissue also contribute to enhanced insulin sensitivity (43, 46). Indeed, we found that pioglitazone treatment substantially affected the expression of key genes related to lipogenesis, lipolysis, or mitochondrial function in these tissues (Figure 3E and Supplemental Figure 3). In our study, KO of miR-223 did not completely block the improvement in insulin sensitivity effected by PPARγ. This is due to the diverse functions of PPARγ and its importance in various cell types and tissues (43, 46).

In summary, we reveal that the PPARγ/miR-223 regulatory axis is crucial in controlling the activation status of ATMs and subsequent adipose tissue inflammation (Figure 8E). miR-223 and its target genes *Rasa1* and *Nfat5* act as critical downstream components of the PPARγ-mediated signaling pathway that regulates ATM activation. Furthermore, identification of the miR-223 target genes *Rasa1* and *Nfat5* in this context provides new gene targets for the development of drugs to mitigate obesity-related diseases.

Methods

Animal experiments. The generation of miR-223–deficient (*Mir223*-KO) mice has been described previously (47). *Mir223*-KO mice were backcrossed onto B6 SJL-*Ptprc Pepc*/BoyJ mice for at least 5 generations. WT C57BL/6J mice were used as controls. All mice were maintained on a 12-hour light/12-hour dark cycle. Five- to six-week-old male mice were fed an HFD (60% fat calories, 20% protein calories, and 20% carbohydrate calories) ad libitum. After 12 weeks of feeding, either pioglitazone (10 mg/kg/day) (48) or saline was administered to the HFD-fed mice via intragastric injection for 4 weeks. After the feeding regimen, mice were subjected to phenotype characterization and metabolic assays, including measurement of metabolic parameters in plasma, as well as insulin and glucose tolerance tests.

Isolation of stromal cells, mature adipocytes, and macrophages from VAT. VATs were mechanically dissected and then digested with 2 mg/ml collagenase II (Invitrogen) for 30 minutes at 37°C. After removing rbc, cells were filtered through a 200-μm cell strainer. Visceral fat stromal cells (VSCs) and mature adipocytes were separated by centrifugation at 1,000 *g* for 5 minutes. To purify ATMs, VSCs were incubated with a biotin-labeled Ab against F4/80 (catalog 13-4801-85; eBioscience) for identification of macrophages. Magnetic beads conjugated with streptavidin (catalog 557812; BD Biosciences) were applied for isolation of macrophages.

Macrophage differentiation and polarization. BMDMs were prepared as previously described (49). Macrophage maturation was examined by flow cytometry with Abs against F4/80 and CD11b. BMDMs were stimulated with LPS (100 ng/ml) for M1 activation or IL-4 (20 ng/ml) for M2 macrophage activation. To enhance activation of PPARγ, BMDMs were treated with pioglitazone (1 μM) (ACTOS, Takeda Pharmaceuti-

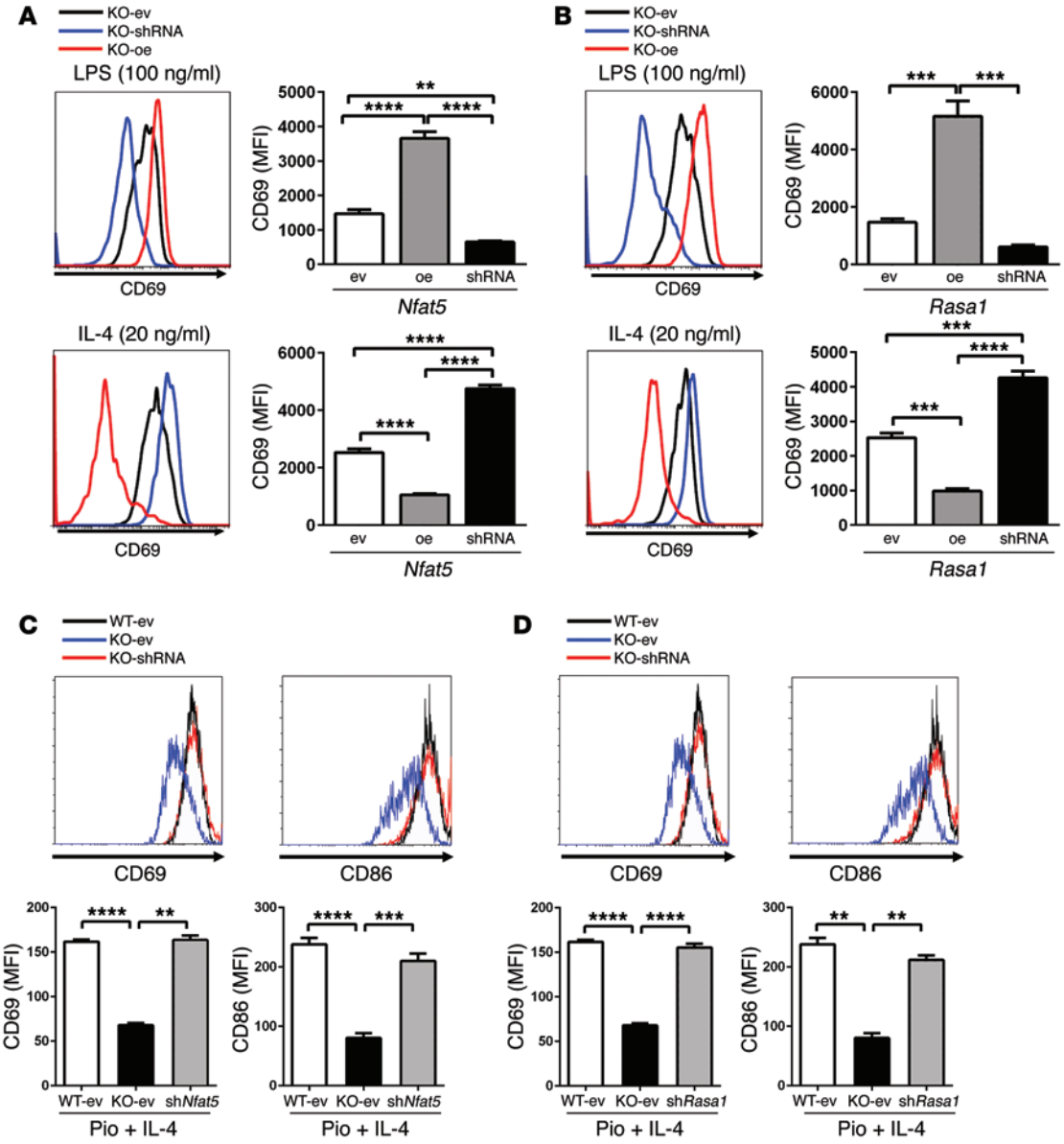

Figure 8. miR-223 controls M2 macrophage activation through modulation of multiple target genes. (**A** and **B**) Production of the activation-related surface marker CD69 in *Mir223*-KO BMDMs with knockdown or overexpression of *Nfat5* and *Rasa1* in the presence of LPS or IL-4 for 48 hours ($n = 4$). ev, *Mir223*-KO BMDMs transfected with empty vector; oe, overexpression of miR-223. (**C** and **D**) Expression of M2 activation–related cell-surface markers CD69 and CD86 in BMDMs after knockdown of *Nfat5* or *Rasa1* in the presence of pioglitazone and IL-4. WT-ev, WT BMDMs transfected with empty vector; KO-ev, *Mir223*-KO BMDMs transfected with empty vector. (**E**) Schematic model of the PPARγ/miR-223–regulatory axis in a macrophage. PPARγ acts as an enhancer to promote the expression of miR-223 through interaction with PPREs. miR-223 is required for PPARγ action in inducing M2 macrophage responses by controlling expression of the target genes *Nfat5* and *Rasa1*. In addition, miR-223 directly suppresses *Pknox1* expression, which leads to inhibition of M1 response. RXR, retinoid X receptor. Data are presented as the mean ± SEM. $^{**}P < 0.01$, $^{***}P < 0.001$, and $^{****}P < 0.0001$ by 1-way ANOVA with Bonferroni's post test.

cals) (50). BMDMs were treated with a PPARγ antagonist, GW9662 (0.1 μM) (Cayman Chemical) to suppress activation of PPARγ.

Flow cytometric analysis. Unless otherwise specified, Abs were purchased from eBioscience. VSCs, ATMs, and BMDMs were stained with fluorescence-tagged Abs to detect cell lineages. Myeloid cells were detected using Abs against F4/80 (catalog 53-4801-82), CD11b (catalog 17-0112-83), and Gr-1 (catalog 45-5931-80); macrophage subtypes were detected with Abs against F4/80, CD11b, CD206 (catalog 141706; BioLegend), and CD11c (catalog 12-0114-83). Macrophage activation was measured with Abs against CD80 (catalog 12-0801-85), CD69 (catalog 45-0691-82), and CD86 (catalog 17-0862-82). Data were analyzed using FlowJo software or Accuri C6 software (BD Biosciences) or Kaluza software (Beckman Coulter).

qPCR analysis. Total RNA was extracted from VATs, ATMs, adipocytes, and BMDMs using the TRIzol extraction protocol according to the manufacturer's instructions (Zymo Research). Gene expression analysis was performed using an iScript One-Step RT-PCR kit with SYBR Green (Bio-Rad) on a Bio-Rad CFX384 Touch Real-Time PCR Detection System. The data presented correspond to the mean of $2^{-\Delta\Delta Ct}$ from at least 3 independent experiments after normalization to β-actin.

ChIP assays. ChIP assays were performed as described previously (51). Briefly, BMDMs were cross-linked for 10 minutes with 1% formaldehyde and quenched with 125 mM glycine. After nuclei were isolated by centrifugation, the pellet was resuspended in lysis buffer containing 0.1% SDS and sonicated to achieve fragment sizes of 200 to 600 bp. The IP was conducted with ChIP-grade protein G magnetic beads using an Ab against PPARγ (catalog ab45036; Abcam). IgG protein (catalog ab18413; Abcam) was used as the negative control. To validate the enrichment, qPCR was performed with tiled primers.

Bio-Plex protein expression assay. The concentrations of TNF-α, IL-1β, and IFN-γ in plasma were determined using a Bio-Plex Cytokine Assay (catalog M60-009RDPD; Bio-Rad). The insulin concentration in plasma was determined using the Bio-Plex Pro Mouse Diabetes Insulin Set (catalog 171-G7006M; Bio-Rad). The abundance of total and phosphorylated AKT (p-AKT) (catalog 171-V50001M) or JNK (catalog 171-V50003M) and p-P65 in VAT was determined using Bio-Plex Cell Signaling Magnetic Assays (all from Bio-Rad). β-actin (catalog 171-V60020M; Bio-Rad) was used as the internal control. These assays were performed using the Bio-Plex MAGPIX Multiplex Reader (Bio-Rad). Results were analyzed using Bio-Plex Data Pro software (Bio-Rad).

IHC. Tissues collected from HFD-fed mice were fixed and stained with Abs against F4/80 (catalog 14-4801-82; eBioscience) to detect macrophages. Ig protein was used as the negative control. Images were captured using a Zeiss Stallion Dual Detector Imaging System with Intelligent Imaging Innovations Software (Carl Zeiss).

Western blotting. After visceral stromal cell isolation, total protein was extracted from VAT or BMDMs using lysis buffer (Cell Signaling Technology). Protein concentrations were determined by Bradford assay. Proteins were separated on PROTEAN TGX Stain-Free Precast Gel (Bio-Rad) and transferred onto a PVDF membrane, followed by detection using Abs directed against NFAT5 (catalog ab56997; Abcam) or RASA1 (catalog ab40677; Abcam) or against total AKT (catalog 9272; Cell Signaling Technology) and p-AKT (catalog 9271; Cell Signaling Technology).

Luciferase reporter assay. The luciferase reporter assay was carried out as described previously (18). To verify that PPARγ binds to the upstream region of pre–miR-223, a 1732-bp DNA fragment (–3849 to –2117 relative to the 5′ end) within the upstream region of pre–miR-223 was inserted upstream of the SV40 promoter of the pGL3 promoter vector (Promega). Luciferase activity was determined by transient transfection of the murine macrophage cell line RAW264.7 with a Bright-Glo Luciferase Reporter Assay System (Promega) and normalized to the internal control firefly luciferase activity. The full 3′-UTR sequence of these genes or at least the 250-bp flanking region of the predicted miR-223–binding site was cloned into a psiCHECK-2 Vector (Promega) downstream of the *Renilla* luciferase–coding region. To validate the suppressive effects of miR-223, the reporter constructs were cotransfected with miR-223 mimic oligonucleotides or negative control oligonucleotides into HEK293 cells. After 48 hours of cotransfection, *Renilla* luciferase activity was measured using the Dual-Glo Luciferase Reporter Assay System (Promega) and normalized to the internal control firefly luciferase activity. Repressive effects of miR-223 on target genes were plotted as the percentage of repression in 3 biological repeats that each contained 3 technical replicates.

Lentiviral shRNA assay. The pLKO.1-CMV-TurboGFP vector (Sigma-Aldrich) with inserted shRNA (targeting *Nfat5* and *Rasa1*) was cotransfected with compatible packaging plasmids into HEK293T cells. The lentiviral supernatants were collected after 72 hours of transfection and used to infect BMDMs. The empty vector was used as the control.

Ectopic expression assays. To overexpress miR-223, a 500-bp length DNA fragment harboring pre–miR-223 was inserted downstream of U6 promoter of the pLB construct. To overexpress *Nfat5* and *Rasa1*, the ORF sequence was inserted downstream of the CMV promoter of the XZ201 plasmid. These constructs were delivered into target cells by transient transfection with X-tremeGENE HP DNA Transfection Reagent (Roche Diagnostics). The empty vectors were used as the control. Overexpression of miR-223, *Nfat5*, and *Rasa1* was validated by either qPCR or Western blot analysis (Supplemental Figure 6).

Statistics. Results are expressed as the mean ± SEM. Each data point derived from qPCR assays represents an average of 2 technical replicates, and data were averaged over independently replicated experiments (n = 3–4 independently collected samples) and analyzed using a 2-tailed Student's t test. The overall group effect was analyzed for significance using 1-way or 2-way ANOVA and Bonferroni's post test for each factor at each individual time point when appropriate. Data analyses were performed using GraphPad Prism, version 6.0 (GraphPad Software). A value of $P < 0.05$ was considered statistically significant.

Study approval. All study protocols were reviewed and approved by the IACUC of Texas A&M University.

Acknowledgments

We are grateful to Deborah J. Kovar of Laboratory Animal Research Resources of Texas A&M University for her assistance with animal care. This work was supported by the American Heart Association (13PRE17050104, to W. Ying); the American Diabetes Association (1-13-JF-59, to B. Zhou); and NIH, National Institute of Diabetes and Digestive and Kidney Diseases (NIDDK) (1R01DK098662, to B. Zhou).

Address correspondence to: Beiyan Zhou, VMR 1197, Room 422b. Department of Physiology and Pharmacology, MS 4466, College of Veterinary Medicine and Biomedical Sciences, Texas A&M University, College Station, Texas 77843, USA. Phone: 979.845.7175; E-mail: bzhou@cvm.tamu.edu.

1. Mills CD, Kincaid K, Alt JM, Heilman MJ, Hill AM. M-1/M-2 macrophages and the Th1/Th2 paradigm. *J Immunol*. 2000;164(12):6166–6173.
2. Lumeng CN, Bodzin JL, Saltiel AR. Obesity induces a phenotypic switch in adipose tissue macrophage polarization. *J Clin Invest*. 2007;117(1):175–184.
3. Lumeng CN, Deyoung SM, Bodzin JL, Saltiel AR. Increased inflammatory properties of adipose tissue macrophages recruited during diet-induced obesity. *Diabetes*. 2007;56(1):16–23.
4. Shi H, Kokoeva MV, Inouye K, Tzameli I, Yin H, Flier JS. TLR4 links innate immunity and fatty acid-induced insulin resistance. *J Clin Invest*. 2006;116(11):3015–3025.
5. Stein M, Keshav S, Harris N, Gordon S. Interleukin 4 potently enhances murine macrophage mannose receptor activity: A marker of alternative immunologic macrophage activation. *J Exp Med*. 1992;176(1):287–292.
6. Odegaard JI, et al. Macrophage-specific PPARγ controls alternative activation and improves insulin resistance. *Nature*. 2007;447(7148):1116–1121.
7. Lumeng CN, Saltiel AR. Inflammatory links between obesity and metabolic disease. *J Clin Invest*. 2011;121(6):2111–2117.
8. McNelis JC, Olefsky JM. Macrophages, immunity, and metabolic disease. *Immunity*. 2014;41(1):36–48.
9. Weisberg SP, McCann D, Desai M, Rosenbaum M, Leibel RL, Ferrante AW. Obesity is associated with macrophage accumulation in adipose tissue. *J Clin Invest*. 2003;112(12):1796–1808.
10. Straus DS, et al. 15-Deoxy-Δ12,14-prostaglandin J2 inhibits multiple steps in the NF-κB signaling pathway. *Proc Natl Acad Sci U S A*. 2000;97(9):4844–4849.
11. Rossi A, et al. Anti-inflammatory cyclopentenone prostaglandins are direct inhibitors of Ikb kinase. *Nature*. 2000;403(6765):103–108.
12. Castrillo A, Diaz-Guerra MJ, Hortelano S, Martin-Sanz P, Bosca L. Inhibition of IκB kinase and IκB phosphorylation by 15-deoxy-Δ(12,14)-prostaglandin J(2) in activated murine macrophages. *Mol Cell Biol*. 2000;20(5):1692–1698.
13. Chawla A, Barak Y, Nagy L, Liao D, Tontonoz P, Evans RM. PPAR-γ dependent and independent effects on macrophage-gene expression in lipid metabolism and inflammation. *Nat Med*. 2001;7(1):48–52.
14. Moore KJ, et al. The role of PPAR-γ in macrophage differentiation and cholesterol uptake. *Nat Med*. 2001;7(1):41–47.
15. Rigamonti E, Chinetti-Gbaguidi G, Staels B. Regulation of macrophage functions by PPAR-α, PPAR-γ, and LXRs in mice and men. *Arterioscler Thromb Vasc Biol*. 2008;28(6):1050–1059.
16. Chinetti G, et al. PPAR-α and PPAR-γ activators induce cholesterol removal from human macrophage foam cells through stimulation of the ABCA1 pathway. *Nat Med*. 2001;7(1):53–58.
17. Bouhlel MA, et al. PPAR gamma activation primes human monocytes into alternative M2 macrophages with anti-inflammatory properties. *Cell Metab*. 2007;6(2):137–143.
18. Zhuang GQ, et al. A novel regulator of macrophage activation miR-223 in obesity-associated adipose tissue inflammation. *Circulation*. 2012;125(23):2892–2903.
19. Olefsky JM, Saltiel AR. PPARγ and the treatment of insulin resistance. *Trends Endocrinol Metab*. 2000;11(9):362–368.
20. Sugii S, et al. PPARγ activation in adipocytes is sufficient for systemic insulin sensitization. *Proc Natl Acad Sci U S A*. 2009;106(52):22504–22509.
21. Hevener AL, et al. Muscle-specific PPARγ deletion causes insulin resistance. *Nat Med*. 2003;9(12):1491–1497.
22. Sandelin A, Alkema W, Engstrom P, Wasserman WW, Lenhard B. Jaspar: An open-access database for eukaryotic transcription factor binding profiles. *Nucleic Acids Res*. 2004; 32(Database issue):91–94.
23. Ferré P. The biology of peroxisome proliferator-activated receptors: relationship with lipid metabolism and insulin sensitivity. *Diabetes*. 2004;53(suppl 1):S43–S50.
24. Berger J, Moller DE. The mechanisms of action of PPARs. *Annu Rev Med*. 2002;53:409–435.
25. Pott S, Kamrani NK, Bourque G, Pettersson S, Liu ET. PPARG binding landscapes in macrophages suggest a genome-wide contribution of PU.1 to divergent PPARG binding in human and mouse. *PLoS One*. 2012;7(10):e48102.
26. Bartel DP. MicroRNAs: Genomics, biogenesis, mechanism, and function. *Cell*. 2004;116(2):281–297.
27. Bartel DP. MicroRNAs: Target recognition and regulatory functions. *Cell*. 2009;136(2):215–233.
28. Krek A, et al. Combinatorial microRNA target predictions. *Nat Genet*. 2005;37(5):495–500.
29. Lewis BP, Burge CB, Bartel DP. Conserved seed pairing, often flanked by adenosines, indicates that thousands of human genes are microRNA targets. *Cell*. 2005;120(1):15–20.
30. Lopez-Rodriguez C, Aramburu J, Jin L, Rakeman AS, Michino M, Rao A. Bridging the NFAT and NFκB families: Nfat5 dimerization regulates cytokine gene transcription in response to osmotic stress. *Immunity*. 2001;15(1):47–58.
31. Oliver JA, Lapinski PE, Lubeck BA, et al. The Ras GTPase-activaing protein neurofibromin 1 promotes the positive selection of thymocytes. *Mol Immunol*. 2013;55(3–4):292–302.
32. Chawla A. Control of macrophage activation and function by PPARs. *Circ Res*. 2010;106(10):1559–1569.
33. Ivashkiv LB. Epigenetic regulation of macrophage polarization and function. *Trends Immunol*. 2013;34(5):216–223.
34. Suganami T, Ogawa Y. Adipose tissue macrophages: Their role in adipose tissue remodeling. *J Leukoc Biol*. 2010;88(1):33–39.
35. Sun K, Kusminski CM, Scherer PE. Adipose tissue remodeling and obesity. *J Clin Invest*. 2011;121(6):2094–2101.
36. Dalmas E, Clement K, Guerre-Millo M. Defining macrophage phenotype and function in adipose tissue. *Trends Immunol*. 2011;32(7):307–314.
37. Cinti S, et al. Adipocyte death defines macrophage localization and function in adipose tissue of obese mice and humans. *J Lipid Res*. 2005;46(11):2347–2355.
38. Nishimura S, et al. In vivo imaging in mice reveals local cell dynamics and inflammation in obese adipose tissue. *J Clin Invest*. 2008;118(2):710–721.
39. Strissel KJ, et al. Adipocyte death, adipose tissue remodeling, and obesity complications. *Diabetes*. 2007;56(12):2910–2918.
40. Kosteli A, et al. Weight loss and lipolysis promote a dynamic immune response in murine adipose tissue. *J Clin Invest*. 2010;120(10):3466–3479.
41. Shaul ME, Bennett G, Strissel KJ, Greenberg AS, Obin MS. Dynamic, M2-like remodeling phenotypes of CD11c+ adipose tissue macrophages during high-fat diet-induced obesity in mice. *Diabetes*. 2010;59(5):1171–1181.
42. Fujisaka S, et al. Regulatory mechanisms for adipose tissue M1 and m2 macrophages in diet-induced obese mice. *Diabetes*. 2009;58(11):2574–2582.
43. de Souza CJ, Eckhardt M, Gagen K, et al. Effects of pioglitazone on adipose tissue remodeling within the setting of obesity and insulin resistance. *Diabetes*. 2001;50(8):1863–1871.
44. Nakamura T, et al. Pioglitazone exerts protective effects against stroke in stroke-prone spontaneously hypertensive rats, independently of blood pressure. *Stroke*. 2007;38(11):3016–3022.
45. Miyazaki Y, Matsuda M, DeFronzo RA. Dose-response effect of pioglitazone on insulin sensitivity and insulin secretion in type 2 diabetes. *Diabetes Care*. 2002;25(3):517–523.
46. Rasouli N, et al. Pioglitazone improves insulin sensitivity through reduction in muscle lipid and redistribution of lipid into adipose tissue. *Am J Physiol Endocrinol Metab*. 2005;288(5):E930–E934.
47. Johnnidis JB, et al. Regulation of progenitor cell proliferation and granulocyte function by microRNA-223. *Nature*. 2008;451(7182):1125–1129.
48. Larsen PJ, et al. Combination of the insulin sensitizer, pioglitazone, and the long-acting GLP-1 human analog, liraglutide, exerts potent synergistic glucose-lowering efficacy in severely diabetic ZDF rats. *Diabetes Obes Metab*. 2008;10(4):301–311.
49. Ying W, Cheruku PS, Bazer FW, Safe SH, Zhou B. Investigation of macrophage polarization using bone marrow derived macrophages. *J Vis Exp*. 2013;76(76):e50323.
50. Aizawa Y, Kawabe J, Hasebe N, Takehara N, Kikuchi K. Pioglitazone enhances cytokine-induced apoptosis in vascular smooth muscle cells and reduces intimal hyperplasia. *Circulation*. 2001;104(4):455–460.
51. Lee TI, Johnstone SE, Young RA. Chromatin immunoprecipitation and microarray-based analysis of protein location. *Nat Protoc*. 2006;1(2):729–748.